First observation of $\gamma\gamma \to p\bar{p}K^+K^-$ and search for exotic baryons in pK systems

C. P. Shen,[2] C. Z. Yuan,[23] I. Adachi,[16,12] H. Aihara,[70] D. M. Asner,[55] V. Aulchenko,[4,53] T. Aushev,[43] R. Ayad,[63] V. Babu,[64] I. Badhrees,[63,30] A. M. Bakich,[62] E. Barberio,[40] P. Behera,[21] V. Bhardwaj,[18] B. Bhuyan,[20] J. Biswal,[27] A. Bobrov,[4,53] G. Bonvicini,[76] A. Bozek,[50] M. Bračko,[38,27] T. E. Browder,[15] D. Červenkov,[5] P. Chang,[49] V. Chekelian,[39] A. Chen,[47] B. G. Cheon,[14] K. Chilikin,[35,42] R. Chistov,[35,42] K. Cho,[31] V. Chobanova,[39] S.-K. Choi,[13] Y. Choi,[61] D. Cinabro,[76] J. Dalseno,[39,65] M. Danilov,[42,35] N. Dash,[19] Z. Doležal,[5] Z. Drásal,[5] D. Dutta,[64] S. Eidelman,[4,53] W. X. Fang,[2] J. E. Fast,[55] T. Ferber,[8] B. G. Fulsom,[55] V. Gaur,[64] N. Gabyshev,[4,53] A. Garmash,[4,53] R. Gillard,[76] R. Glattauer,[24] P. Goldenzweig,[29] O. Grzymkowska,[50] J. Haba,[16,12] K. Hayasaka,[51] H. Hayashii,[46] W.-S. Hou,[49] T. Iijima,[45,44] K. Inami,[44] G. Inguglia,[8] A. Ishikawa,[68] R. Itoh,[16,12] Y. Iwasaki,[16] I. Jaegle,[15] H. B. Jeon,[33] K. K. Joo,[6] T. Julius,[40] K. H. Kang,[33] E. Kato,[68] C. Kiesling,[39] D. Y. Kim,[60] J. B. Kim,[32] K. T. Kim,[32] S. H. Kim,[14] Y. J. Kim,[31] P. Kodyš,[5] S. Korpar,[38,27] D. Kotchetkov,[15] P. Križan,[36,27] P. Krokovny,[4,53] A. Kuzmin,[4,53] Y.-J. Kwon,[78] J. S. Lange,[10] C. H. Li,[40] H. Li,[22] L. Li,[57] Y. Li,[75] L. Li Gioi,[39] J. Libby,[21] D. Liventsev,[75,16] M. Lubej,[27] T. Luo,[56] M. Masuda,[69] T. Matsuda,[41] D. Matvienko,[4,53] K. Miyabayashi,[46] H. Miyata,[51] R. Mizuk,[35,42,43] G. B. Mohanty,[64] S. Mohanty,[64,74] A. Moll,[39,65] H. K. Moon,[32] R. Mussa,[26] E. Nakano,[54] M. Nakao,[16,12] T. Nanut,[27] K. J. Nath,[20] Z. Natkaniec,[50] S. Nishida,[16,12] S. Ogawa,[67] S. L. Olsen,[58] W. Ostrowicz,[50] P. Pakhlov,[35,42] G. Pakhlova,[35,43] B. Pal,[7] C.-S. Park,[78] H. Park,[33] L. Pesántez,[3] R. Pestotnik,[27] M. Petrič,[27] L. E. Piilonen,[75] C. Pulvermacher,[29] J. Rauch,[66] M. Ritter,[37] Y. Sakai,[16,12] S. Sandilya,[7] L. Santelj,[16] T. Sanuki,[68] V. Savinov,[56] T. Schlüter,[37] O. Schneider,[34] G. Schnell,[1,17] C. Schwanda,[24] Y. Seino,[51] D. Semmler,[10] K. Senyo,[77] I. S. Seong,[15] M. E. Sevior,[40] T.-A. Shibata,[71] J.-G. Shiu,[49] B. Shwartz,[4,53] F. Simon,[39,65] A. Sokolov,[25] E. Solovieva,[35,43] S. Stanič,[52] M. Starič,[27] J. F. Strube,[55] J. Stypula,[50] M. Sumihama,[11] T. Sumiyoshi,[72] M. Takizawa,[59] U. Tamponi,[26,73] K. Tanida,[58] F. Tenchini,[40] K. Trabelsi,[16,12] M. Uchida,[71] S. Uehara,[16,12] T. Uglov,[35,43] Y. Unno,[14] S. Uno,[16,12] P. Urquijo,[40] Y. Usov,[4,53] C. Van Hulse,[1] G. Varner,[15] C. H. Wang,[48] M.-Z. Wang,[49] P. Wang,[23] M. Watanabe,[51] Y. Watanabe,[28] K. M. Williams,[75] E. Won,[32] J. Yamaoka,[55] J. Yelton,[9] Y. Yook,[78] Y. Yusa,[51] C. C. Zhang,[23] Z. P. Zhang,[57] V. Zhilich,[4,53] V. Zhukova,[42] V. Zhulanov,[4,53] and A. Zupanc[36,27]

(Belle Collaboration)

[1]*University of the Basque Country UPV/EHU, 48080 Bilbao*
[2]*Beihang University, Beijing 100191*
[3]*University of Bonn, 53115 Bonn*
[4]*Budker Institute of Nuclear Physics SB RAS, Novosibirsk 630090*
[5]*Faculty of Mathematics and Physics, Charles University, 121 16 Prague*
[6]*Chonnam National University, Kwangju 660-701*
[7]*University of Cincinnati, Cincinnati, Ohio 45221*
[8]*Deutsches Elektronen–Synchrotron, 22607 Hamburg*
[9]*University of Florida, Gainesville, Florida 32611*
[10]*Justus-Liebig-Universität Gießen, 35392 Gießen*
[11]*Gifu University, Gifu 501-1193*
[12]*SOKENDAI (The Graduate University for Advanced Studies), Hayama 240-0193*
[13]*Gyeongsang National University, Chinju 660-701*
[14]*Hanyang University, Seoul 133-791*
[15]*University of Hawaii, Honolulu, Hawaii 96822*
[16]*High Energy Accelerator Research Organization (KEK), Tsukuba 305-0801*
[17]*IKERBASQUE, Basque Foundation for Science, 48013 Bilbao*
[18]*Indian Institute of Science Education and Research Mohali, SAS Nagar, 140306*
[19]*Indian Institute of Technology Bhubaneswar, Satya Nagar 751007*
[20]*Indian Institute of Technology Guwahati, Assam 781039*
[21]*Indian Institute of Technology Madras, Chennai 600036*
[22]*Indiana University, Bloomington, Indiana 47408*
[23]*Institute of High Energy Physics, Chinese Academy of Sciences, Beijing 100049*
[24]*Institute of High Energy Physics, Vienna 1050*
[25]*Institute for High Energy Physics, Protvino 142281*
[26]*INFN—Sezione di Torino, 10125 Torino*
[27]*J. Stefan Institute, 1000 Ljubljana*
[28]*Kanagawa University, Yokohama 221-8686*
[29]*Institut für Experimentelle Kernphysik, Karlsruher Institut für Technologie, 76131 Karlsruhe*
[30]*King Abdulaziz City for Science and Technology, Riyadh 11442*
[31]*Korea Institute of Science and Technology Information, Daejeon 305-806*

[32]*Korea University, Seoul 136-713*
[33]*Kyungpook National University, Daegu 702-701*
[34]*École Polytechnique Fédérale de Lausanne (EPFL), Lausanne 1015*
[35]*P.N. Lebedev Physical Institute of the Russian Academy of Sciences, Moscow 119991*
[36]*Faculty of Mathematics and Physics, University of Ljubljana, 1000 Ljubljana*
[37]*Ludwig Maximilians University, 80539 Munich*
[38]*University of Maribor, 2000 Maribor*
[39]*Max-Planck-Institut für Physik, 80805 München*
[40]*School of Physics, University of Melbourne, Victoria 3010*
[41]*University of Miyazaki, Miyazaki 889-2192*
[42]*Moscow Physical Engineering Institute, Moscow 115409*
[43]*Moscow Institute of Physics and Technology, Moscow Region 141700*
[44]*Graduate School of Science, Nagoya University, Nagoya 464-8602*
[45]*Kobayashi-Maskawa Institute, Nagoya University, Nagoya 464-8602*
[46]*Nara Women's University, Nara 630-8506*
[47]*National Central University, Chung-li 32054*
[48]*National United University, Miao Li 36003*
[49]*Department of Physics, National Taiwan University, Taipei 10617*
[50]*H. Niewodniczanski Institute of Nuclear Physics, Krakow 31-342*
[51]*Niigata University, Niigata 950-2181*
[52]*University of Nova Gorica, 5000 Nova Gorica*
[53]*Novosibirsk State University, Novosibirsk 630090*
[54]*Osaka City University, Osaka 558-8585*
[55]*Pacific Northwest National Laboratory, Richland, Washington 99352*
[56]*University of Pittsburgh, Pittsburgh, Pennsylvania 15260*
[57]*University of Science and Technology of China, Hefei 230026*
[58]*Seoul National University, Seoul 151-742*
[59]*Showa Pharmaceutical University, Tokyo 194-8543*
[60]*Soongsil University, Seoul 156-743*
[61]*Sungkyunkwan University, Suwon 440-746*
[62]*School of Physics, University of Sydney, New South Wales 2006*
[63]*Department of Physics, Faculty of Science, University of Tabuk, Tabuk 71451*
[64]*Tata Institute of Fundamental Research, Mumbai 400005*
[65]*Excellence Cluster Universe, Technische Universität München, 85748 Garching*
[66]*Department of Physics, Technische Universität München, 85748 Garching*
[67]*Toho University, Funabashi 274-8510*
[68]*Department of Physics, Tohoku University, Sendai 980-8578*
[69]*Earthquake Research Institute, University of Tokyo, Tokyo 113-0032*
[70]*Department of Physics, University of Tokyo, Tokyo 113-0033*
[71]*Tokyo Institute of Technology, Tokyo 152-8550*
[72]*Tokyo Metropolitan University, Tokyo 192-0397*
[73]*University of Torino, 10124 Torino*
[74]*Utkal University, Bhubaneswar 751004*
[75]*Virginia Polytechnic Institute and State University, Blacksburg, Virginia 24061*
[76]*Wayne State University, Detroit, Michigan 48202*
[77]*Yamagata University, Yamagata 990-8560*
[78]*Yonsei University, Seoul 120-749*

(Received 9 April 2016; published 30 June 2016)

The process $\gamma\gamma \to p\overline{p}K^+K^-$ and its intermediate processes are measured for the first time using a 980 fb^{-1} data sample collected with the Belle detector at the KEKB asymmetric-energy e^+e^- collider. The production of $p\overline{p}K^+K^-$ and a $\Lambda(1520)^0$ ($\overline{\Lambda}(1520)^0$) signal in the pK^- ($\overline{p}K^+$) invariant mass spectrum are clearly observed. However, no evidence for an exotic baryon near 1540 MeV/c^2, denoted as $\Theta(1540)^0$ ($\overline{\Theta}(1540)^0$) or $\Theta(1540)^{++}$ ($\Theta(1540)^{--}$), is seen in the pK^- ($\overline{p}K^+$) or pK^+ ($\overline{p}K^-$) invariant mass spectra. Cross sections for $\gamma\gamma \to p\overline{p}K^+K^-$, $\Lambda(1520)^0\overline{p}K^+ + \text{c.c.}$ and the products $\sigma(\gamma\gamma \to \Theta(1540)^0\overline{p}K^+ + \text{c.c.})\mathcal{B}(\Theta(1540)^0 \to pK^-)$ and $\sigma(\gamma\gamma \to \Theta(1540)^{++}\overline{p}K^- + \text{c.c.})\mathcal{B}(\Theta(1540)^{++} \to pK^+)$ are measured. We also determine upper limits on the products of the χ_{c0} and χ_{c2} two-photon decay widths and their branching fractions to $p\overline{p}K^+K^-$ at the 90% credibility level.

DOI: 10.1103/PhysRevD.93.112017

Quantum chromodynamics allows for the existence of exotic hadronic states such as glueballs, hybrids and multiquark states with valence quark and gluon configurations that are distinct from normal quark-antiquark mesons and three-quark baryons [1]. There is a long history of searches for these types of states, but no solid examples were seen prior to the recent discovery of tetraquark and pentaquark states containing charm and beauty quarks.

A charged charmoniumlike state $Z(4430)^{\pm}$ was observed by the Belle experiment in 2007 in the $\pi^{\pm}\psi'$ system produced in B decays [2]. In addition to the $Z(4430)^{\pm}$, recently BESIII and Belle also observed a series of charged Z states such as the $Z(3900)^{\pm}$ [3], $Z(4020)^{\pm}$ [4], $Z(4200)^{\pm}$ [5], $Z(4050)^{\pm}$ and $Z(4250)^{\pm}$ [6]. As such, a charged state must contain at least four quarks; these Z states have been interpreted either as tetraquark states, molecular states, or other configurations [7].

Very recently, the LHCb Collaboration reported the observation of two exotic structures, denoted as $P_c(4380)^+$ and $P_c(4450)^+$, in the $J/\psi p$ system in $\Lambda_b^0 \to J/\psi K^- p$ [8]. Since the valence structure of $J/\psi p$ is $c\bar{c}uud$, the newly discovered particles must consist of at least five quarks. Several theoretical interpretations of these states have been developed, such as the diquark picture [9] and hadronic molecules [10]. Actually, the first strong experimental evidence for a pentaquark state, referred to as the $\Theta(1540)^+$, was reported in the reaction $\gamma n \to nK^+K^-$ in the LEPS experiment [11]. It was a candidate for a $uudd\bar{s}$ pentaquark state. However, it was not confirmed in larger-statistics data samples in the same experiment and was most probably not a genuine state [12].

To confirm the pentaquark states discovered by LHCb, further experimental searches for exotic baryons should be pursued. If fully confirmed, exotic baryons would be most naturally explained as pentaquark states. The possibility of observing additional hypothetical exotic baryons in $\gamma\gamma$ collisions is discussed in Ref. [13], where Fig. 3 depicts possible diagrams for the exclusive double- and single-pentaquark productions in $\gamma\gamma$ collisions. High luminosity electron-positron colliders are well suited to measurements of the two-photon production since they provide a large flux of quasireal photons colliding at two-photon center-of-mass (CM) energies covering a wide range. Due to the high luminosity accumulated at B factories, searches for exotic baryons in exclusive $\gamma\gamma$ reactions are possible. The authors in Ref. [13] suggest that single pentaquark production may be viewed as a collision of a nonresonant di-baryon and a di-meson pair. One of the incoming photons fluctuates into two mesons with strangeness; one meson then collides with the hadronic system produced by the other incoming photon. The cross section for the reaction $\gamma\gamma \to p\bar{p}K^+K^-$ is predicted to be around 0.1 nb for $W_{\gamma\gamma} \geq 2(m_p + m_K)$ [13], where $W_{\gamma\gamma}$ is the CM energy of two-photon system that is the same as the invariant mass of the final-state hadron system and m_p and m_K are the proton and kaon nominal masses [14]. This presents the opportunity to search for novel exotic baryons, denoted as $\Theta(1540)^0 \to pK^-$ and $\Theta(1540)^{++} \to pK^+$ which are similar to $\Theta(1540)^+$, in intermediate processes in two-photon annihilations.

Here, we report the cross sections for $\gamma\gamma \to p\bar{p}K^+K^-$ through the measurement of $e^+e^- \to (e^+e^-)p\bar{p}K^+K^-$, as well as searches for possible exotic baryons as intermediate states. The results are based on an analysis of a 980 fb^{-1} data sample taken at or near the $\Upsilon(nS)$ $(n = 1, \ldots, 5)$ resonances with the Belle detector [15] operating at the KEKB asymmetric-energy e^+e^- collider [16]. The analysis is made in the "zero-tag" mode, where neither the recoil electron nor positron is detected. We restrict the virtuality of the incident photons to be small by imposing a strict transverse-momentum balance along the beam axis for the final state hadronic system.

The detector, which is described in detail elsewhere [15], is a large-solid-angle magnetic spectrometer that consists of a silicon vertex detector, a 50-layer central drift chamber, an array of aerogel threshold Cherenkov counters, a barrel-like arrangement of time-of-flight scintillation counters, and an electromagnetic calorimeter comprised of CsI(Tl) crystals located inside a superconducting solenoid coil that provides a 1.5 T magnetic field. An iron flux-return located outside of the coil is instrumented to detect K_L^0 mesons and to identify muons.

We use the program TREPS [17] to generate signal Monte Carlo (MC) events and determine experimental efficiencies and effective luminosities for photon-photon collisions. In this generator, the two-photon luminosity function is calculated and events are generated at a specified $\gamma\gamma$ CM energy ($W_{\gamma\gamma}$) using the equivalent photon approximation [18]. The efficiencies for detecting $\gamma\gamma \to p\bar{p}K^+K^-$ and its intermediate processes $\Lambda(1520)^0\bar{p}K^+$, $\Theta(1540)^0\bar{p}K^+$ and $\Theta(1540)^{++}\bar{p}K^-$ [19] at different fixed $W_{\gamma\gamma}$ values are determined by assuming a phase space model. The width of the $\Theta(1540)$ for the nominal results is set to 9.7 MeV from Ref. [12].

We require four reconstructed charged tracks with zero net charge. For these tracks, the impact parameters perpendicular to and along the beam direction with respect to the interaction point are required to be less than 0.5 cm and 4 cm, respectively, and the transverse momentum in the laboratory frame is restricted to be higher than 0.1 GeV/c. For each charged track, information from different detector subsystems is combined to form a likelihood $\mathcal{L}_i$ for each particle species [20]. Tracks of interest with $\mathcal{R}_K = \mathcal{L}_K/(\mathcal{L}_K + \mathcal{L}_\pi) > 0.6$ are identified as kaons with an efficiency of about 91%; about 5.9% of the pions are misidentified as kaons. A track with $\mathcal{R}_{p/\bar{p}} = \mathcal{L}_{p/\bar{p}}/(\mathcal{L}_{p/\bar{p}} + \mathcal{L}_\pi) > 0.6$ and $\mathcal{R}_{p/\bar{p}} = \mathcal{L}_{p/\bar{p}}/(\mathcal{L}_{p/\bar{p}} + \mathcal{L}_K) > 0.6$ is identified as a proton or antiproton with an efficiency of about 95%. A similar likelihood ratio is formed for electron identification [21]. Photon conversion

backgrounds are removed by vetoing any charged track in the event that is identified as electron or positron ($\mathcal{R}_e > 0.9$); this requirement keeps more than 98.5% of the signals.

There are some obvious $e^+e^- \to p\bar{p}K^+K^-$ backgrounds from initial state radiation processes observed as a clear peak at around zero in the distribution of the square of the missing mass recoiling against the four charged tracks $p\bar{p}K^+K^-$ ($M^2_{\rm miss}$). We require $M^2_{\rm miss} > 4\ ({\rm GeV}/c^2)^2$ to remove such backgrounds. To suppress backgrounds with extra neutral clusters in the final state, events are removed if there are one or more additional photons with energy greater than 150 MeV.

The magnitude of the vector sum of the four transverse momenta in the e^+e^- CM frame, $|\sum \vec{P}^*_t|$, which approximates the transverse momentum of the two-photon-collision system, is used as a discriminating variable to separate signal from background. The signal tends to accumulate at small $|\sum \vec{P}^*_t|$ values while the non-$\gamma\gamma$ background is distributed over a wider range. The $|\sum \vec{P}^*_t|$ distribution for the whole $p\bar{p}K^+K^-$ mass region for the selected events is shown in Fig. 1. This distribution is fitted with a signal shape determined from MC simulation and a first-order Chebyshev polynomial to represent the background from non-$\gamma\gamma$ processes. To check possible peaking backgrounds, inclusive MC samples of $e^+e^- \to q\bar{q}$ ($q = u, d, c, s$), $\tau^+\tau^-$ and $B\bar{B}$ are analyzed. The shaded histogram in Fig. 1 shows the normalized background contribution after all selection criteria are applied, which is consistent with the total background estimated from the fit.

We obtain the number of $p\bar{p}K^+K^-$ events in each $p\bar{p}K^+K^-$ invariant mass bin ($n^{\rm fit}$) by fitting the $|\sum \vec{P}^*_t|$ distribution between zero and 1.0 GeV/c. The signal shape is obtained from MC simulation in the corresponding mass bin and the background shape is parameterized as a first-order Chebyshev polynomial. The background shape is fixed to that from the overall fit due to the small statistics in each mass bin. The resulting $p\bar{p}K^+K^-$ invariant mass distribution is shown in Fig. 2(a).

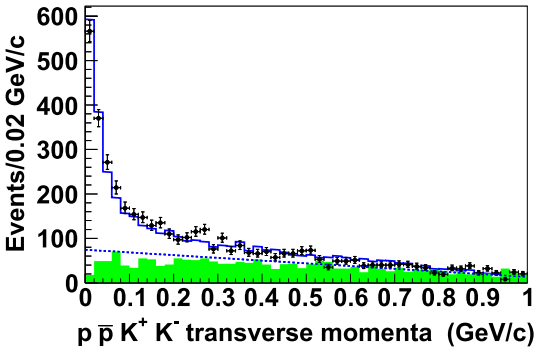

FIG. 1. The magnitude of the transverse momentum of the $p\bar{p}K^+K^-$ system with respect to the beam direction in the e^+e^- CM frame for the selected $p\bar{p}K^+K^-$ events over the entire mass region. Points with error bars are data. The solid histogram is the fitted result, the dashed line is the total background estimate and the shaded histogram is the normalized contribution from inclusive MC samples described in the text.

The cross section $\sigma_{\gamma\gamma\to p\bar{p}K^+K^-}(W_{\gamma\gamma})$ is calculated from

$$\sigma_{\gamma\gamma\to p\bar{p}K^+K^-}(W_{\gamma\gamma}) = \frac{n^{\rm fit}}{\frac{dL_{\gamma\gamma}}{dW_{\gamma\gamma}}\epsilon(W_{\gamma\gamma})\Delta W_{\gamma\gamma}}, \qquad (1)$$

where $\frac{dL_{\gamma\gamma}}{dW_{\gamma\gamma}}$ is the differential luminosity of the two-photon collision, ϵ is the efficiency, $\Delta W_{\gamma\gamma}$ is the bin width, and $n^{\rm fit}$ is the number of signal events in the $\Delta W_{\gamma\gamma}$ bin.

The $\gamma\gamma \to p\bar{p}K^+K^-$ cross section is shown in Fig. 2(b), where the errors are statistical only. No clear structure is seen in this distribution and the largest value is around 40 pb, which is lower than the rough estimate of 100 pb from Ref. [13].

To search for Kp intermediate states, we require transverse momentum balance for the $p\bar{p}K^+K^-$ system by imposing $|\sum \vec{P}^*_t| < 0.17$ GeV/c, which was optimized by maximizing the value of $S/\sqrt{S+B}$. Here, S is the number of fitted $\Lambda(1520)^0$ signal events and B is the number of fitted background events in the $\Lambda(1520)^0$ signal region. Distributions of $M(pK^-)$ vs $M(\bar{p}K^+)$ and $M(pK^+)$ vs $M(\bar{p}K^-)$ for the selected $p\bar{p}K^+K^-$ events are shown in

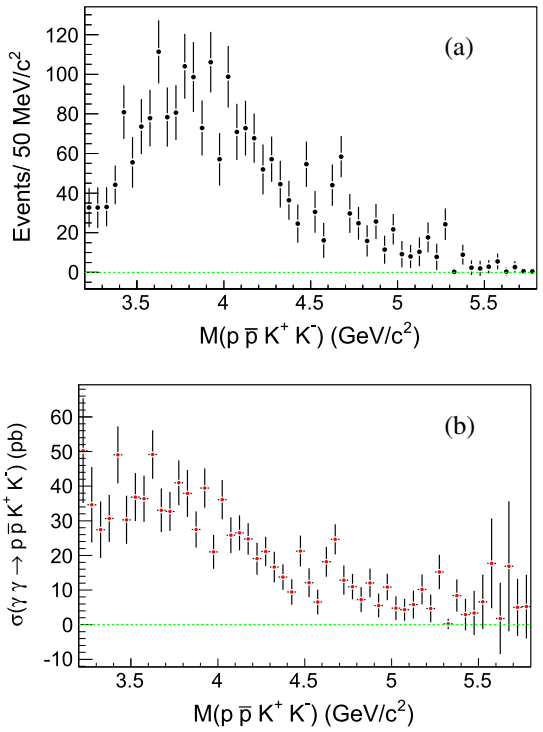

FIG. 2. (a) The $p\bar{p}K^+K^-$ invariant mass distribution obtained by fitting the $|\sum \vec{P}^*_t|$ distributions in each $p\bar{p}K^+K^-$ mass bin and (b) the cross section of $\gamma\gamma \to p\bar{p}K^+K^-$ in each $p\bar{p}K^+K^-$ mass bin. The error bars are statistical only.

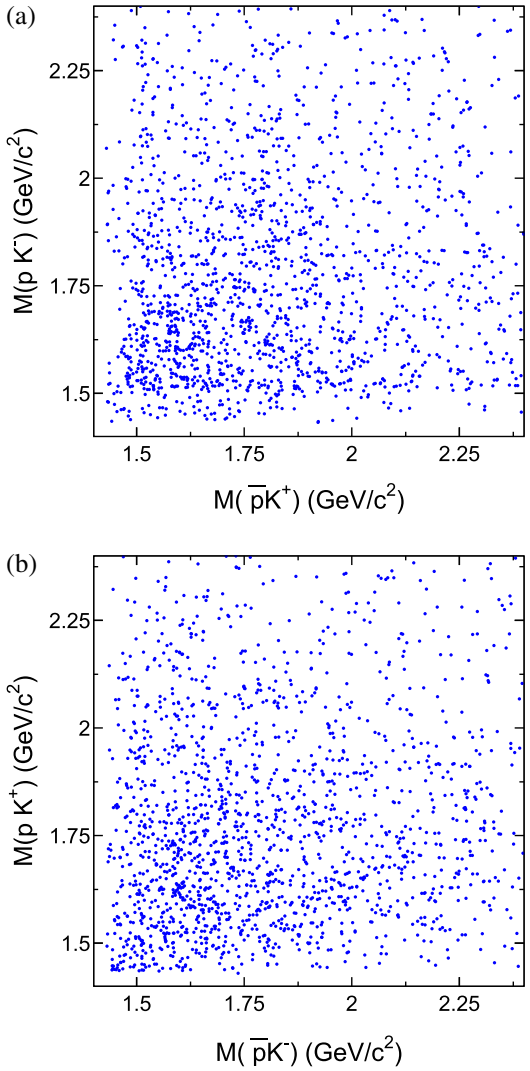

FIG. 3. The distributions of (a) $M(pK^-)$ versus $M(\bar{p}K^+)$ and (b) $M(pK^+)$ versus $M(\bar{p}K^-)$ for the selected $\gamma\gamma \to p\bar{p}K^+K^-$ candidate events.

Fig. 3. Horizontal and vertical bands can be seen in Fig. 3(a) directions at around 1.52 GeV/c^2, corresponding to $\Lambda(1520)^0 \to pK^-$ and $\overline{\Lambda}(1520)^0 \to \overline{p}K^+$ decays in the former plot. No signals are seen for $\Theta(1540)^0 \to pK^-$ nor $\Theta(1540)^{++} \to pK^+$ in either scatter plot.

Figure 4 shows the pK^- and pK^+ invariant mass distributions, where for the $M(pK^+)$ distribution the pK^- mass is required to be outside the $\Lambda(1520)^0$ signal region between 1.49 and 1.55 GeV/c^2. To extract the signal and background yields in the $|\sum \vec{P}_t^*|$ signal region and the corresponding sideband region, defined as 0.6 GeV/$c < |\sum \vec{P}_t^*| <$ 1.0 GeV/c, unbinned maximum likelihood fits to the pK^- invariant mass distributions are performed simultaneously. The shapes of the $\Lambda(1520)^0$ and $\Theta(1540)^0$ signals with mass resolutions of 6.5 MeV/c^2 are obtained from MC simulations with energy-dependent widths and phase space factors included. In the fit, a

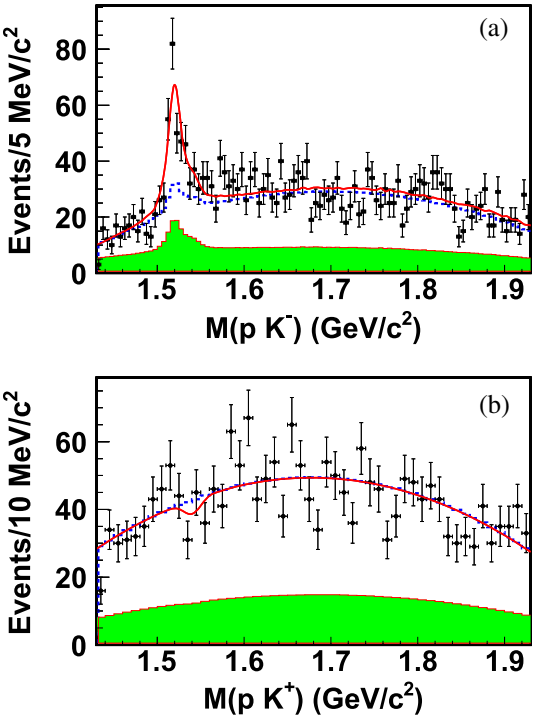

FIG. 4. The fits to the (a) pK^- and (b) pK^+ invariant mass distributions for the (a) $\Lambda(1520)^0$, $\Theta(1540)^0$ and (b) $\Theta(1540)^{++}$ candidates in the whole $p\bar{p}K^+K^-$ mass region. The solid lines show the results of the simultaneous fits described in the text, the dotted curves show the total background estimates, and the shaded histograms are the normalized $|\sum \vec{P}_t^*|$ sideband contributions.

second-order Chebyshev polynomial is used for the backgrounds in addition to the normalized $|\sum \vec{P}_t^*|$ sideband contribution. Similar fits with a $\Theta(1540)^{++}$ signal are performed to the pK^+ invariant mass distributions. Figure 4(a) shows the fitted results to the $M(pK^-)$ distribution with the $\Lambda(1520)^0$ and $\Theta(1540)^0$ signal shapes included, while Fig. 4(b) shows the fitted results to the $M(pK^+)$ distribution with the $\Theta(1540)^{++}$ signal shape included only. From the fits, the numbers of $\Lambda(1520)^0$, $\Theta(1540)^0$ and $\Theta(1540)^{++}$ signal events are 288 ± 48, 22 ± 34 and -16 ± 34, respectively. The statistical significances of the $\Lambda(1520)^0$ and $\Theta(1540)^0$ are estimated to be 8.6σ and 1.4σ, respectively, by calculating $\sqrt{-2\ln(\mathcal{L}_0/\mathcal{L}_{\rm max})}$, where $\mathcal{L}_0$ and $\mathcal{L}_{\rm max}$ are the likelihoods of the fits without and with the signal component, respectively.

We obtain the yields of $\Lambda(1520)^0\overline{p}K^+$ and $\Theta(1540)^0\overline{p}K^+$ in each $p\overline{p}K^+K^-$ invariant mass bin by performing similar simultaneous fits to $M(pK^-)$ distribution as was done above for the entire $p\overline{p}K^+K^-$ mass region. The resulting $\Lambda(1520)^0\overline{p}K^+$ and $\Theta(1540)^0\overline{p}K^+$ invariant mass distributions are shown in Figs. 5(a) and 5(b). The corresponding $\sigma(\gamma\gamma \to \Lambda(1520)^0\overline{p}K^+)$ and $\sigma(\gamma\gamma \to \Theta(1540)^0\overline{p}K^+)\mathcal{B}(\Theta(1540)^0 \to pK^-)$ measurements are

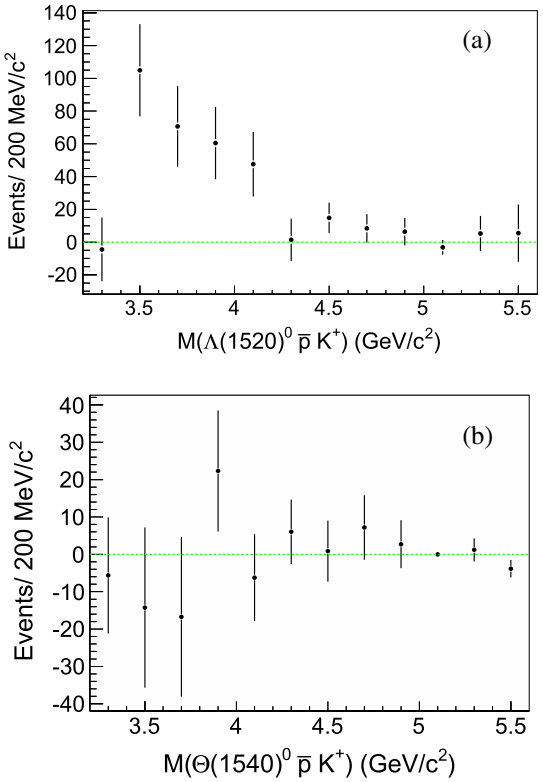

FIG. 5. The (a) $\Lambda(1520)^0\bar{p}K^+$ and (b) $\Theta(1540)^0\bar{p}K^+$ invariant mass distributions obtained by fitting the pK^- invariant mass distribution simultaneously to the $|\sum \vec{P}_t^*|$ signal region and sideband in each $p\bar{p}K^+K^-$ mass bin.

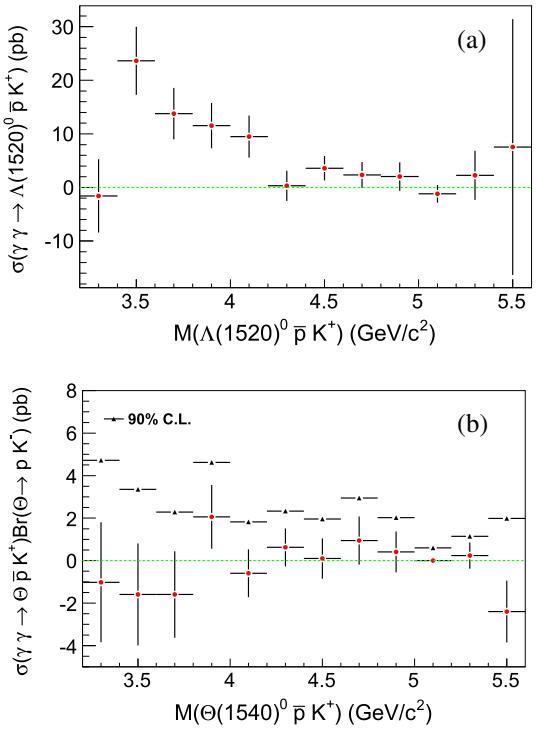

FIG. 6. The measurements of (a) $\sigma(\gamma\gamma \to \Lambda(1520)^0\bar{p}K^+)$ and (b) $\sigma(\gamma\gamma \to \Theta(1540)^0\bar{p}K^+)$ $\mathcal{B}(\Theta(1540)^0 \to pK^-)$ are shown as points with error bars. The error bars are statistical only. The corresponding 90% C.L. upper limits are shown with triangles.

shown in Figs. 6(a) and 6(b), where the error bars are statistical only. Since no $\Theta(1540)^0$ signal is observed, the upper limits on the product $\sigma(\gamma\gamma \to \Theta(1540)^0\overline{p}K^+)\mathcal{B}(\Theta(1540)^0 \to pK^-)$ are shown in Fig. 6(b) with triangles at the 90% credibility level (C.L.), where the upper limit on the signal yield ($N_{\rm up}$) in each $\Theta(1540)^0\overline{p}K^+$ mass bin is determined by solving the equation $\int_0^{N_{\rm up}} \mathcal{L}(x)dx / \int_0^{+\infty} \mathcal{L}(x)dx = 0.9$ [22], where x is the number of fitted signal events and $\mathcal{L}(x)$ is the likelihood function in the fit to the data, convolved with a Gaussian function whose width equals the total systematic uncertainty.

With a similar method, the number of $\Theta(1540)^{++}\overline{p}K^-$ signal events in each $p\overline{p}K^+K^-$ invariant mass bin is obtained from similar simultaneous fits to the $M(pK^+)$ distribution. The resulting $\Theta(1540)^{++}\overline{p}K^-$ invariant mass distribution and the corresponding $\sigma(\gamma\gamma \to \Theta(1540)^{++}\overline{p}K^-)\mathcal{B}(\Theta(1540)^{++} \to pK^+)$ product values, together with the upper limits at the 90% C.L., are shown in Figs. 7(a) and 7(b).

Figure 8(a) shows the K^+K^- invariant mass distribution of the selected candidate events, where a clear ϕ signal is observed. An unbinned extended maximum likelihood fit is applied with a Gaussian resolution function with free parameters as the ϕ signal shape and a first-order polynomial as the background shape. From the fit, we obtain 88 ± 12 ϕ signal events. The ϕ signal region is defined as the ± 8 MeV/c^2 interval around the ϕ nominal mass [14], as indicated by the arrows in Fig. 8(a), and ϕ sidebands are defined as $1.002\,\text{GeV}/c^2 < M(K^+K^-) < 1.010\,\text{GeV}/c^2$ or $1.030\,\text{GeV}/c^2 < M(K^+K^-) < 1.038\,\text{GeV}/c^2$. The $\phi p\overline{p}$ invariant mass distribution within the ϕ signal region is shown in Fig. 8(b), where the shaded histogram is from the normalized ϕ-sideband events. There are no evident structures. The sum of the ϕp and $\phi\overline{p}$ invariant mass distributions is shown in Fig. 8(c). No significant evidence of an $s\overline{s}$ partner of the pentaquark states $P_c(4380)$ and $P_c(4450)$ [8] is observed.

Systematic error sources and their contributions to the cross section measurements are summarized in Table I. The particle identification uncertainties are 1.4% for each kaon and 2.4% (2.0%) for each proton (antiproton). A momentum-weighted systematic error in tracking efficiency of about 0.4% is taken for each track. The statistical error in the MC samples is about 0.5%. The accuracy of the two-photon luminosity function calculated with the TREPS generator is estimated to be about 5%, including the error from neglecting radiative corrections (2%), the uncertainty from the form factor effect (2%) [17], and the uncertainty in the total integrated luminosity (1.4%). The trigger efficiency for four-charged-track events is rather high because of the redundancy of the Belle first-level multitrack trigger.

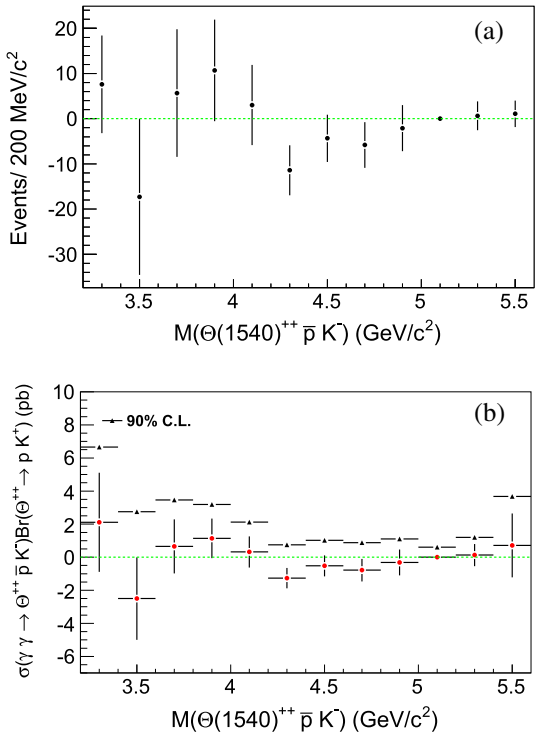

FIG. 7. (a) The $\Theta(1540)^{++}\bar{p}K^-$ invariant mass distribution obtained by fitting the pK^+ invariant mass distribution simultaneously to the $|\sum \vec{P}_t^*|$ signal region and sideband in each $p\bar{p}K^+K^-$ mass bin and (b) the measurements of $\sigma(\gamma\gamma \to \Theta(1540)^{++}\bar{p}K^-)\mathcal{B}(\Theta(1540)^{++} \to pK^+)$ shown as points with error bars. The error bars are statistical only. The corresponding 90% C.L. upper limits are shown with triangles.

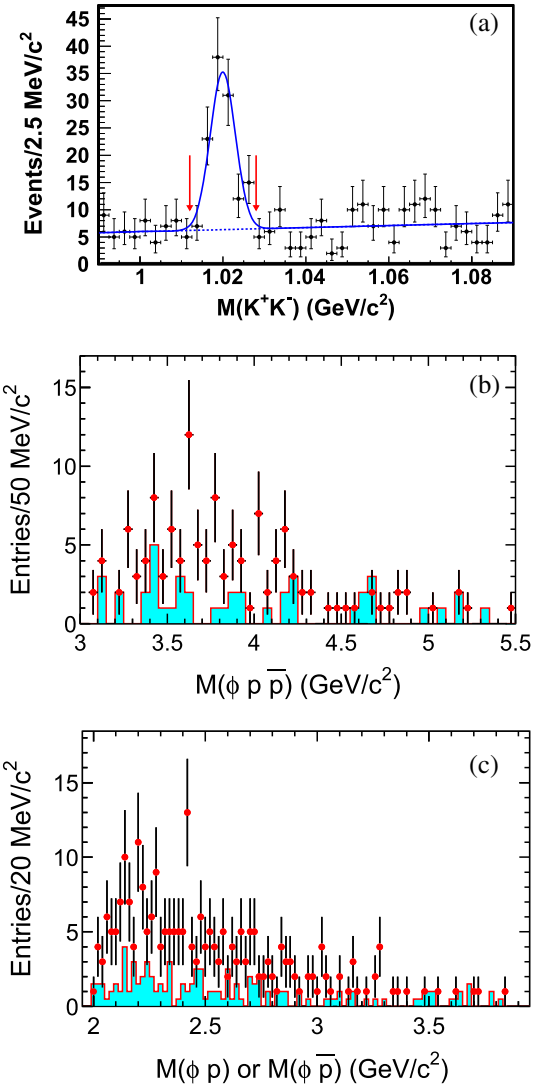

FIG. 8. The (a) K^+K^-, (b) $\phi p\bar{p}$, and (c) the sum of the ϕp and $\phi\bar{p}$ invariant mass spectra. The arrows in (a) indicate the ϕ signal region. The shaded histograms in (b) and (c) are from the normalized ϕ-sideband events.

According to the MC simulation, the signal trigger efficiency increases with the $p\overline{p}K^+K^-$ mass. The uncertainty of the trigger simulation is less than 4% [23]. The preselection efficiency for the final states has little dependence on the $p\overline{p}K^+K^-$ invariant mass, with an uncertainty smaller than 2.5%. From Ref. [14], the uncertainty in the world average value for $\mathcal{B}(\Lambda(1520)^0 \to pK^-)$ is 2.3%. The uncertainty in the fitted yield for the signal is estimated by varying the background shape and fit range, which is 8.1% for $p\overline{p}K^+K^-$, 9.8% for $\Lambda(1520)^0\overline{p}K^+$, 40% for $\Theta(1540)^0\overline{p}K^+$, and 21% for $\Theta(1540)^{++}\overline{p}K^-$. For the $\Lambda(1520)^0\overline{p}K^+$, $\Theta(1540)^0\overline{p}K^+$ and $\Theta(1540)^{++}\overline{p}K^-$ modes, we estimate the systematic errors associated with the $\Lambda(1520)^0$ and $\Theta(1540)$ resonance parameters by changing the values of the masses and widths of the resonances by $\pm 1\sigma$. The resulting differences of 5.7%, 7.4% and 5.5% in the fitted results are taken as systematic errors. The uncertainty on the mass resolution is estimated by changing the MC signal resolution by ±10%, which is 1.1% for $\Lambda(1520)^0\overline{p}K^+$, 2.5% for $\Theta(1540)^0\overline{p}K^+$ and 4.0% for $\Theta(1540)^{++}\overline{p}K^-$. Assuming that all of these systematic error sources are independent, we add them in quadrature to obtain the total systematic errors of 13%, 16%, 42% and

TABLE I. Relative systematic errors (%) on the cross section measurements for $\gamma\gamma \to p\bar{p}K^+K^-$, $\Lambda(1520)^0\bar{p}K^+$, $\Theta(1540)^0\bar{p}K^+$ and $\Theta(1540)^{++}\bar{p}K^-$, respectively.

Source	$p\bar{p}K^+K^-$	$\Lambda(1520)^0$	Θ^0	Θ^{++}
Part. identification	7.2	7.2	7.2	7.2
Tracking	1.6	1.6	1.6	1.6
MC statistics	0.5	0.5	0.5	0.5
Lum. function	5.0	5.0	5.0	5.0
Trigger efficiency	4.0	4.0	4.0	4.0
Preselection efficiency	2.5	2.5	2.5	2.5
Branching fractions	···	2.3	···	···
Fit uncertainty	8.1	9.8	40	21
Res. parameters	···	5.7	7.4	5.5
Signal resolution	···	1.1	2.5	4.0
Sum	13	16	42	25

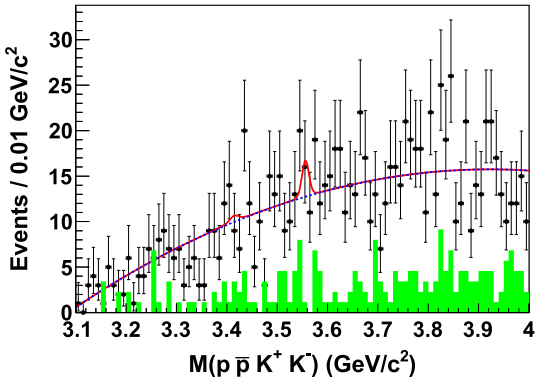

FIG. 9. The invariant mass distribution of $p\bar{p}K^+K^-$ in the charmonium mass region with the requirement $|\sum \vec{P}_t^*| < 0.17$ GeV/c. The shaded histogram is the normalized $|\sum \vec{P}_t^*|$ sideband contribution. The points with error bars are data, the dashed line is the fitted total background and the solid curve is the best fit.

25% for $p\overline{p}K^+K^-$, $\Lambda(1520)^0\overline{p}K^+$, $\Theta(1540)^0\overline{p}K^+$ and $\Theta(1540)^{++}\overline{p}K^-$, respectively.

For a $p\overline{p}K^+K^-$ invariant mass above 3.1 GeV/c^2, we measure the production rate of charmonium states. In measuring the production rates, $|\sum \vec{P}_t^*|$ is required to be less than 0.17 GeV/c in order to reduce backgrounds from non-two-photon processes and two-photon processes with extra particles other than the signal final state.

Figure 9 shows the $p\overline{p}K^+K^-$ invariant mass distribution. No clear χ_{c0} or χ_{c2} signals are seen. The mass spectrum is fitted with two incoherent Breit-Wigner functions convolved with a corresponding Gaussian resolution function as the χ_{c0} and χ_{c2} signal shapes, and a second-order Chebyshev polynomial as the background shape. The fit result is shown in Fig. 9 as a solid curve, where the dashed line is the fitted background and the shaded histogram is the normalized $|\sum \vec{P}_t^*|$ sideband contribution. The statistical signal significances are 0.2σ and 0.8σ for the χ_{c0} and χ_{c2}, respectively.

Since no significant signals are observed, the 90% C.L. upper limits on the χ_{c0} and χ_{c2} yields are determined to be 16.4 and 18.0, respectively. In these calculations, we assume there is no interference between the charmonium and the continuum amplitudes. A systematic error estimate similar to that for the cross sections results in total systematic errors of 29% and 13% for $\Gamma_{\gamma\gamma}(R)\mathcal{B}(R \to p\overline{p}K^+K^-)$ for $R = \chi_{c0}$ and χ_{c2}, respectively.

The product of the two-photon decay width and branching fraction is obtained from the relation $\Gamma_{\gamma\gamma}(R)\mathcal{B}(R \to \text{final state}) = N/[(2J+1)\epsilon\mathcal{K}\mathcal{L}_{\text{int}}]$, where N is the number of observed events, ϵ is the efficiency, J is the spin of the resonance, and $\mathcal{L}_{\text{int}}$ is the integrated luminosity. The factor $\mathcal{K}$ is calculated from the two-photon luminosity function $\mathcal{L}_{\gamma\gamma}(M_R)$ for a resonance with mass M_R using the relation $\mathcal{K} = 4\pi^2\mathcal{L}_{\gamma\gamma}(M_R)/M_R^2$, which is valid when the resonance width is small compared to its mass. The $\mathcal{K}$ factor is calculated to be 1.15 and 0.95 fb/eV for the χ_{c0} and χ_{c2}, respectively, using TREPS [17]. The efficiencies are 2.77% and 3.97% for the χ_{c0} and χ_{c2}, respectively. From the above results, we obtain upper limits of 0.53 eV ($J = 0$) and 0.10 eV ($J = 2$) for $\Gamma_{\gamma\gamma}(\chi_{cJ})\mathcal{B}(\chi_{cJ} \to p\overline{p}K^+K^-)$.

In summary, we observe the process $\gamma\gamma \to p\overline{p}K^+K^-$ and search for the first time for possible exotic baryons $\Theta(1540)^0$ and $\Theta(1540)^{++}$ decaying to pK^- and pK^+ in the two-photon process $\gamma\gamma \to p\overline{p}K^+K^-$. Clear $\gamma\gamma \to p\overline{p}K^+K^-$ signals are observed. While the $\Lambda(1520)^0$ signals in the pK^- invariant mass spectrum are also observed, no evidence for any exotic baryon is seen in the pK^- or pK^+ invariant mass spectrum. For all of the above-mentioned processes, the cross sections are measured for the first time. The cross sections for $\gamma\gamma \to p\overline{p}K^+K^-$ are lower by a factor of 2.5 or more than the theoretical prediction of 0.1 nb in Ref. [13]. At the same time, no clear χ_{c0} or χ_{c2} signal is seen in the $p\overline{p}K^+K^-$ invariant mass spectrum, and 90% C.L. upper limits on the products of the two-photon decay width and branching fraction of the χ_{c0} and χ_{c2} to $p\overline{p}K^+K^-$ are established.

We thank the KEKB group for the excellent operation of the accelerator; the KEK cryogenics group for the efficient operation of the solenoid; and the KEK computer group, the National Institute of Informatics, and the PNNL/EMSL computing group for valuable computing and SINET4 network support. We acknowledge support from the Ministry of Education, Culture, Sports, Science, and Technology (MEXT) of Japan, the Japan Society for the Promotion of Science (JSPS), and the Tau-Lepton Physics Research Center of Nagoya University; the Australian Research Council; Austrian Science Fund under Grants No. P 22742-N16 and No. P 26794-N20; the National Natural Science Foundation of China under Contracts No. 10575109, No. 10775142, No. 10875115, No. 11175187, No. 11475187 and No. 11575017; the Chinese Academy of Science Center for Excellence in Particle Physics; the Ministry of Education, Youth and Sports of the Czech Republic under Contract No. LG14034; the Carl Zeiss Foundation, the Deutsche Forschungsgemeinschaft, the Excellence Cluster Universe, and the VolkswagenStiftung; the Department of Science and Technology of India; the Istituto Nazionale di Fisica Nucleare of Italy; the WCU program of the Ministry of Education, National Research Foundation (NRF) of Korea Grants No. 2011-0029457, No. 2012-0008143, No. 2012R1A1A2008330, No. 2013R1A1A3007772, No. 2014R1A2A2A01005286, No. 2014R1A2A2A01002734, No. 2015R1A2A2A01003280, No. 2015H1A2A1033649; the Basic Research Lab program under NRF Grant No. KRF-2011-0020333, Center for Korean J-PARC Users, No. NRF-2013K1A3A7A06056592; the Brain Korea 21-Plus program and Radiation Science Research Institute; the Polish Ministry of Science and Higher Education and the National Science

Center; the Ministry of Education and Science of the Russian Federation and the Russian Foundation for Basic Research; the Slovenian Research Agency; Ikerbasque, Basque Foundation for Science and the Euskal Herriko Unibertsitatea (UPV/EHU) under program UFI 11/55 (Spain); the Swiss National Science Foundation; the Ministry of Education and the Ministry of Science and Technology of Taiwan; and the U.S. Department of Energy and the National Science Foundation. This work is supported by a Grant-in-Aid from MEXT for Science Research in a Priority Area (New Development of Flavor Physics) and from JSPS for Creative Scientific Research (Evolution of Tau-lepton Physics).

[1] M. Gell-Mann, Phys. Lett. **8**, 214 (1964).
[2] S.-K. Choi *et al.* (Belle Collaboration), Phys. Rev. Lett. **100**, 142001 (2008).
[3] M. Ablikim *et al.* (BESIII Collaboration), Phys. Rev. Lett. **110**, 252001 (2013); Z. Q. Liu *et al.* (Belle Collaboration), Phys. Rev. Lett. **110**, 252002 (2013).
[4] M. Ablikim *et al.* (BESIII Collaboration), Phys. Rev. Lett. **111**, 242001 (2013).
[5] K. Chilikin *et al.* (Belle Collaboration), Phys. Rev. D **90**, 112009 (2014).
[6] R. Mizuk *et al.* (Belle Collaboration), Phys. Rev. D **78**, 072004 (2008).
[7] N. Brambilla *et al.*,Eur. Phys. J. C **71**, 1534 (2011); **74**, 2981 (2014).
[8] R. Aaij *et al.* (LHCb Collaboration), Phys. Rev. Lett. **115**, 072001 (2015).
[9] R. F. Lebed, Phys. Lett. B **749**, 454 (2015); L. Maiani, A. D. Polosa, and V. Riquer, Phys. Lett. B **749**, 289 (2015); V. V. Anisovich, M. A. Matveev, J. Nyiri, A. V. Sarantsev, and A. N. Semenova, arXiv:1507.07652; R. Ghosh, A. Bhattacharya, and B. Chakrabarti, arXiv:1508.00356; V. V. Anisovich, M. A. Matveev, J. Nyiri, A. V. Sarantsev, and A. N. Semenova, Int. J. Mod. Phys. A **30**, 1550190 (2015).
[10] H. X. Chen, L. S. Geng, W. H. Liang, E. Oset, E. Wang, and J. J. Xie, Phys. Rev. C **93**, 065203 (2016); R. Chen, X. Liu, X. Q. Li, and S. L. Zhu, Phys. Rev. Lett. **115**, 132002 (2015); L. Roca, J. Nieves, and E. Oset, Phys. Rev. D **92**, 094003 (2015); J. He, Phys. Lett. B **753**, 547 (2016); U. G. Meiner and J. A. Oller, Phys. Lett. B **751**, 59 (2015).
[11] T. Nakano *et al.* (LEPS Collaboration), Phys. Rev. Lett. **91**, 012002 (2003).
[12] T. B. Liu, Y. J. Mao, and B. Q. Ma, Int. J. Mod. Phys. A **29**, 1430020 (2014).
[13] S. Armstrong, B. Mellado, and S. L. Wu, J. Phys. G **30**, 1801 (2004).
[14] K. A. Olive *et al.* (Particle Data Group), Chin. Phys. C **38**, 090001 (2014) and 2015 update.
[15] A. Abashian *et al.* (Belle Collaboration), Nucl. Instrum. Methods Phys. Res., Sect. A **479**, 117 (2002); also, see detector section in J. Brodzicka *et al.*, Prog. Theor. Exp. Phys. (2012) 04D001.
[16] S. Kurokawa and E. Kikutani, Nucl. Instrum. Methods Phys. Res., Sect. A **499**, 1 (2003), and other papers included in this volume; T. Abe *et al.*, Prog. Theor. Exp. Phys. (2013) 03A001 and following articles up to 03A011.
[17] S. Uehara, KEK Report No. 96-11 (1996). In the generator, the form factor is assumed to be $1/(1+Q^2/W^2)$, where Q^2 is a 4-momentum transfer of an electron and represents the virtuality of the photon, http://lss.fnal.gov/archive/other1/kek-report-96-11.pdf.
[18] C. Berger and W. Wagner, Phys. Rep. **146**, 1 (1987).
[19] Charge-conjugate decays are implicitly assumed throughout the paper.
[20] E. Nakano, Nucl. Instrum. Methods Phys. Res., Sect. A **494**, 402 (2002).
[21] K. Hanagaki, H. Kakuno, H. Ikeda, T. Iijima, and T. Tsukamoto, Nucl. Instrum. Methods Phys. Res., Sect. A **485**, 490 (2002).
[22] In common high-energy physics usage, this Bayesian interval has been reported as "confidence interval," which is a frequentist-statistics term.
[23] S. Uehara *et al.* (Belle Collaboration), Eur. Phys. J. C **53**, 1 (2008).